Chemical Science

ROYAL SOCIETY OF CHEMISTRY

EDGE ARTICLE

View Article Online
View Journal

Cite this: DOI: 10.1039/d5sc10121b

All publication charges for this article have been paid for by the Royal Society of Chemistry

Tris((4-BMes$_2$)phenyl)methanide: a carbanion with a delocalised triple quinoidal structure

Yufeng Zhang, [abc] Johannes Krebs,[b] Alexandra Friedrich, [b] Shigehiro Yamaguchi, [c] Ivo Krummenacher, [b] Holger Braunschweig, [b] Todd B. Marder *[b] and Lei Ji *[a]

Received 25th December 2025
Accepted 12th March 2026

DOI: 10.1039/d5sc10121b

rsc.li/chemical-science

Herein, we report that incorporation of strongly electron-accepting BMes$_2$ (Mes = 2,4,6-trimethylphenyl) groups at the three *para*-positions of a trigonal [CPh$_3$]$^-$ framework leads to extensive delocalisation of the negative charge over the three aryl branches and onto the boron centres. Single-crystal structure analysis reveals that all three branches of **CB-Mes-1** exhibit short C(center)–C(phenylene) and C(phenylene)–B bonds, and significant C–C bond length alternation within the central phenylene ring, indicative of a unique triple quinoidal structure in a single system. The HOMO of **CB-Mes-1** is delocalised over the whole molecule, further indicating its quinoidal structure. Upon deprotonation of the neutral HC[(C$_6$H$_4$)-4-B(Mes)$_2$]$_3$ precursor (**CB-Mes**), the resulting **CB-Mes-1** shows a 439 nm (18 400 cm^{-1}) red shift in its absorption from 316 nm in the UV to 755 nm in the NIR. Compared with trigonal N-centred analogues and [CPh$_3$]$^-$, **CB-Mes-1** displays a significantly raised HOMO energy level, accompanied by a dramatic red shift of the maximum absorption band with a large oscillator strength.

Introduction

Unveiling electron delocalisation is fundamental to understanding the structure, reactivity, and properties of organic compounds.[1–13] Trimethylenemethane (TMM), first recognised by Moffitt and Coulson in 1948, is the most typical representative of trigonal systems.[14] It features high symmetry and reactivity, along with a triplet open-shell diradical ground state.[15] Thus, TMM is a representative non-Kekulé system characterised by the presence of at least two atoms not involved in π-bonding, resulting in four unpaired π electrons that are localised rather than delocalised over the entire molecule (Fig. 1a).[16] Shiotani *et al.* reported that the TMM radical cation shows an apparent D_{3h} structure. Nevertheless, this is a result of intramolecular dynamics among the three energetically equivalent C_{2v} structures, and its unpaired electron primarily resides in the π orbitals of the two equivalent terminal carbon atoms.[17] This finding highlights the fact that high molecular symmetry does not necessarily ensure uniform electron delocalisation.

Compared to TMM, the trigonal triphenylmethyl [CPh$_3$] cation, radical, and anion systems (**A**–**C**, respectively, Fig. 1b) are more stable owing to the resonance stabilisation arising from charge delocalisation over the phenyl rings, and offer more peripheral sites for functionalisation.[18,19] In the unsubstituted CPh$_3$ systems, the distances from the central carbon atom to its three neighbouring carbon atoms in these molecules exhibit appreciable double-bond character.[20–22] For [CPh$_3$]$^-$ (**C**), as it interacts with metal cations in most cases, the central carbon atom adopts sp^2 hybridisation and exhibits delocalisation of the negative charge over the phenyl rings.[23–25] However, the "free" [CPh$_3$]$^-$ ([CPh$_3$$^-$][Me$_4N^+$]) exhibits a distinct geometry in the solid state; one phenyl ring is nearly coplanar with the central carbon framework (11.5°), one falls within the expected range (26.1°), and the third is much more twisted with respect to the central plane (61.1°). As a result, the co-planar ring displays a large extent of charge delocalisation, whereas charge delocalisation is nearly shut off for the highly twisted phenyl ring.[26] In terms of the functionalised trigonal [CPh$_3$]$^+$ trityl system, three electron-donating dimethylamino groups at the *para*-positions of the phenyl rings in **A** give rise to a triply quinoidal structure, in which the C–N bond lengths are 1.364 Å (**D**).[27] The central carbon atom of CPh$_3$ systems can be replaced by a boron atom and the aryl rings modified with electron donors. For example, in the trigonal carbazolyl-substituted triarylborane **E**, the ground-state dipole moment of **E** is 1.7 D, and it exhibits a symmetry lower than D_3 in the ground state, as two branches of the molecule contribute only marginally to the overall dipole moment.[28] This demonstrates that the electron-

[a]*State Key Laboratory of Flexible Electronics (LOFE) & Institute of Flexible Electronics (IFE), Northwestern Polytechnical University, 127 West Youyi Road, Xi'an, 710072, China. E-mail: iamlji@nwpu.edu.cn*

[b]*Institute for Inorganic Chemistry and Institute for Sustainable Chemistry & Catalysis with Boron, Julius-Maximilians-Universität Würzburg, Am Hubland, 97074 Würzburg, Germany. E-mail: todd.marder@uni-wuerzburg.de*

[c]*Department of Chemistry, Graduate School of Science, Integrated Research Consortium on Chemical Sciences (IRCCS) and Institute of Transformative Bio-Molecules (WPI-ITbM), Nagoya University, Furo Chikusa, Nagoya 464-8601, Japan*

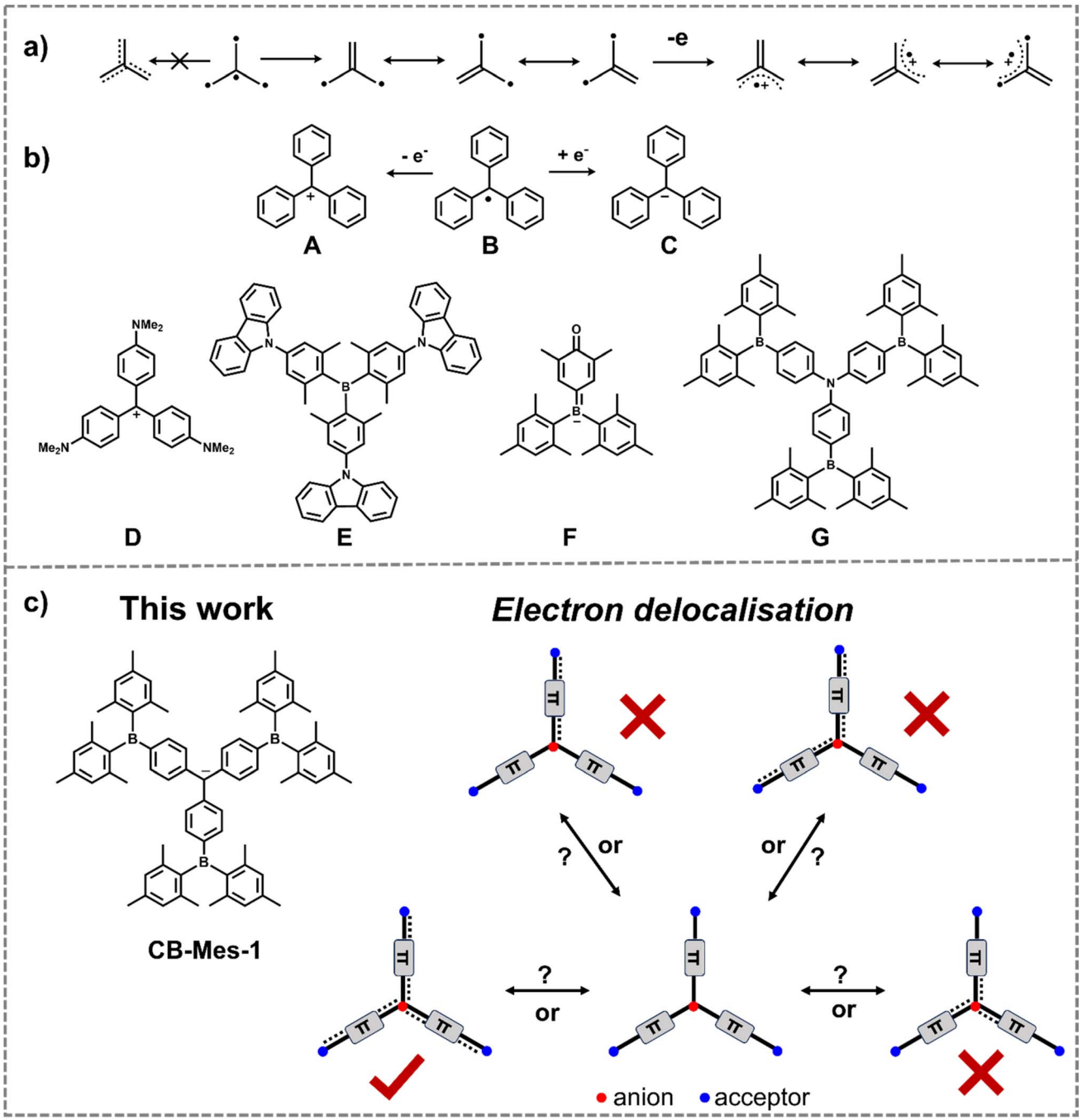

Fig. 1 (a) The Kekulé structures of TMM, and delocalisation pattern of the TMM radical cation (right); (b) [CPh_3] systems (A–D), boron-centred systems (E, F), and nitrogen-centred system (G); (c) the electron delocalisation profile of CB-Mes-1.

donating influence of the carbazolyl substituents does not distribute evenly over the three aryl moieties in this case. The strong electron-donating O^- group at the *para*-position of the phenyl ring attached to the boron centre in **F**, leads to a quinoidal structure, as observed in a few other cases.[29] Likewise, the carbanion $[Mes_2BCH_2]^-$ shows B=C double bond character (Mes = 2,4,6-trimethylphenyl).[22] The NPh_3 core is isoelectronic with $[CPh_3]^-$ and, with three BAr_2 (Ar = –Mes (**G**), –^{F}Mes, and –C_6F_5) groups as strong acceptors, those compounds exhibit delocalised HOMOs.[30,31]

However, no study has clarified how the central negative charge in $[CPh_3]^-$ responds to a simultaneous reduction in the electron density of all three aryl substituents (Fig. 1c). Herein, we installed three strongly π-accepting $BMes_2$ groups[32–37] at the *para*-positions of the phenyl rings in the trigonal $[CPh_3]^-$ framework *via* synthesis of the neutral compound HC[1,4-$C_6H_4B(Mes_2)]_3$, **CB-Mes**, and, following deprotonation, its corresponding carbanion **CB-Mes-1** (Fig. 1c). Structural and electronic properties were elucidated by single-crystal X-ray diffraction, photophysical measurements, and DFT

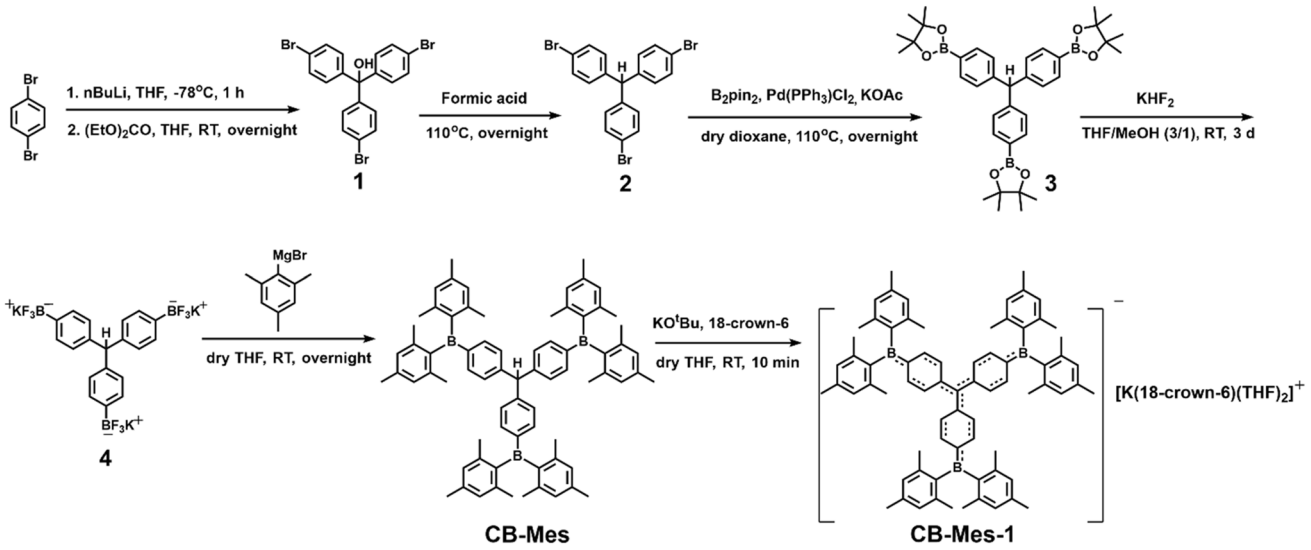

Scheme 1 Synthetic routes to **CB-Mes** and **CB-Mes-1**.

calculations. The results demonstrate that the p_z-electrons on the central carbon atom are fully delocalised over the entire molecule, giving rise to a triple quinoidal resonance structure.

Results and discussion

The synthetic routes to **CB-Mes** and **CB-Mes-1** are shown in Scheme 1. Compounds **1–3** were synthesised according to literature procedures.[38,39] Compound **3** was transformed into its potassium trifluoroborate salt **4** in 94% yield using KHF_2 under an ambient atmosphere in a THF/methanol mixture. It was then reacted with the Grignard reagent MesMgBr to give the neutral **CB-Mes** compound in 14% yield. Owing to the strong electron accepting ability of the $BMes_2$ moieties, the central carbon atom was easily deprotonated by treatment with KO^{t}Bu in THF, affording the corresponding carbanion (**CB-Mes-1**). This process was monitored by *in situ* ^{1}H NMR spectroscopy (Fig. S1). The ^{1}H NMR spectra of **CB-Mes** and **CB-Mes-1** reveal two doublets and one singlet in the aromatic region with an intensity ratio of 1 : 1 : 2, consistent with C_3 symmetry in solution. Interestingly, all proton signals of **CB-Mes-1** shift downfield compared to those of **CB-Mes**. The upfield shift of the ^{11}B NMR signal of **CB-Mes-1** ($\delta = 66.1$ ppm) relative to that of **CB-Mes** ($\delta =$ 73.3 ppm) reveals an increase in the electron density at the three boron centres, indicating the possibility of a triple quinoidal resonance structure.

Single crystals suitable for X-ray diffraction analysis were obtained by slow evaporation of a THF solution of **CB-Mes** and

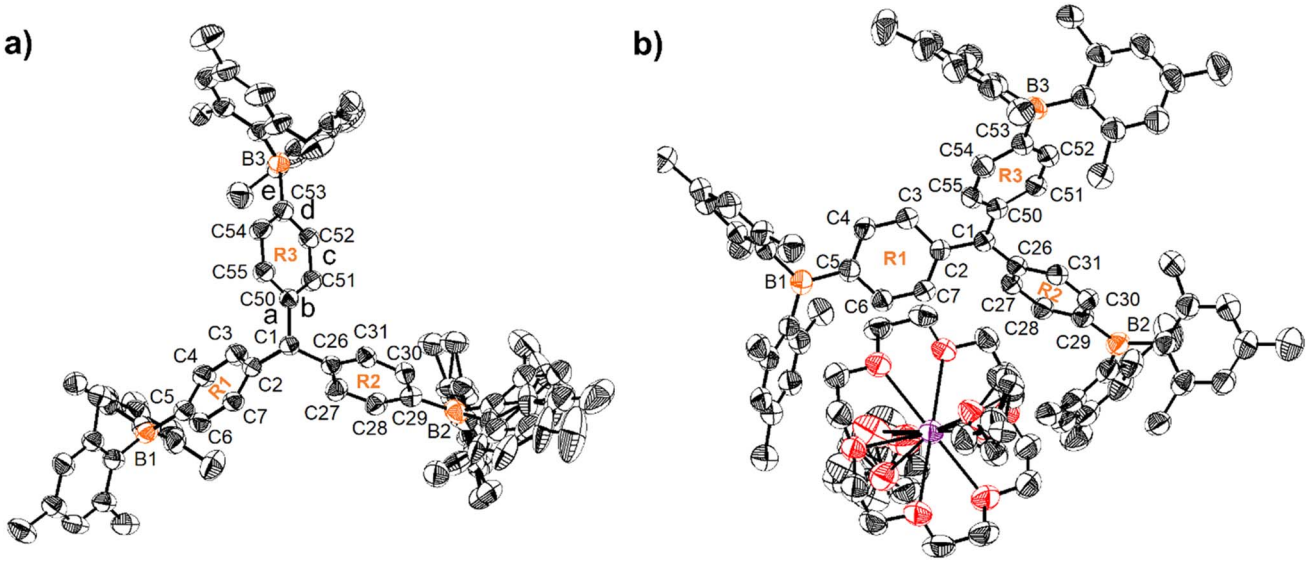

Fig. 2 Molecular structures of (a) **CB-Mes** and (b) **CB-Mes-1**, determined by single-crystal X-ray diffraction with ellipsoids drawn at 50% probability. H atoms and uncoordinated THF molecules are omitted for clarity.

Table 1 Bond lengths [Å], angles [°], dihedral angles [°], and torsion angles between phenylene rings R1, R2, and R3 [°] from single-crystal diffraction data and from DFT calculations on model compounds (calc.)[a]

Compound	CB-Mes	CB-Mes-1
C1–C2	1.518(5)	1.446(4)
C1–C26	1.527(5)	1.449(4)
C1–C50	1.521(4)	1.463(4)
Mean bond length **a**	1.522(3)	1.453(2)
C–C (calc.)	*1.531*	*1.449*
C2–C3	1.395(5)	1.431(4)
C26–C27	1.380(5)	1.409(4)
C50–C51	1.397(5)	1.417(4)
C7–C2	1.395(5)	1.411(4)
C31–C26	1.400(5)	1.423(4)
C55–C50	1.386(5)	1.409(4)
Mean bond length **b**	1.392(2)	1.417(2)
C–C (calc.)	*1.402*	*1.420*
C3–C4	1.377(6)	1.370(4)
C27–C28	1.397(6)	1.376(4)
C51–C52	1.377(5)	1.370(4)
C6–C7	1.388(5)	1.366(4)
C30–C31	1.375(5)	1.374(4)
C54–C55	1.384(5)	1.374(4)
Mean bond length **c**	1.383(2)	1.372(2)
C–C (calc.)	*1.393*	*1.386*
C4–C5	1.411(5)	1.412(4)
C28–C29	1.379(6)	1.419(4)
C52–C53	1.409(5)	1.402(4)
C5–C6	1.410(5)	1.410(4)
C29–C30	1.413(6)	1.404(5)
C53–C54	1.403(5)	1.414(4)
Mean bond length **d**	1.404(2)	1.410(2)
C–C (calc.)	*1.411*	*1.413*
B1–C5	1.555(6)	1.547(5)
B2–C29	1.544(17)[b]	1.545(5)
B3–C53	1.561(5)	1.542(5)
Mean bond length **e**	1.553(6)	1.545(3)
B–C (calc.)	*1.567*	*1.535*
C7–C2–C1–C26	88.0(4)	27.1(5)
C7–C2–C1–C26 (calc.)	*80.4*	*30.6*
C31–C26–C1–C50	72.4(4)	28.4(4)
C31–C26–C1–C50 (calc.)	*80.7*	*30.7*
C55–C50–C1–C2	81.8(4)	27.3(5)
C55–C50–C1–C2 (calc.)	*81.2*	*30.5*
C2–C1–C26	112.2(3)	120.4(3)
C2–C1–C26 (calc.)	*112.9*	*120.0*
C2–C1–C50	111.1(3)	120.3(3)
C2–C1–C50 (calc.)	*112.9*	*120.0*
C26–C1–C50	111.5(3)	119.2(3)
C26–C1–C50 (calc.)	*112.8*	*120.0*
sum of the C–C1–C angles	334.8(2)	359.9(2)
sum of the C–C1–C angles (calc.)	*338.6*	*360.0*
∠(R1,R2)	80.6(1)	52.5(1)
∠(R2,R3)	88.3(1)	50.8(1)
∠(R1,R3)	83.5(1)	45.6(1)

[a] Esd's of the mean values were calculated from the esd's of the individual values using the formula $\sqrt{\sum_{i=1}^{n}\sigma_i^2}/n$. Values obtained from DFT calculations (calc.) employed model compounds **CB-Mes′** and **CB-Mes-1′** in which the Mes groups were replaced with phenyl groups. Bond types **a**, **b**, **c**, **d**, and **e** are shown in Fig. 2a. [b] Values are given for the major part (68% occupancy) of the disorder.

by diffusion of pentane into a THF solution of **CB-Mes-1**, respectively. Their structures are shown in Fig. 2, and selected bond lengths and angles are given in Table 1. **CB-Mes** and **CB-Mes-1** adopt familiar propeller-like geometries, and crystallise in the monoclinic *Cc* and triclinic $P\bar{1}$ space groups, respectively. The torsion angles between the planes of the phenylene rings describing their relative orientations in **CB-Mes** are 80.6(1)°, 88.3(1)°, and 83.5(1)°, which significantly decrease in **CB-Mes-1** to 52.5(1)°, 50.8(1)°, and 45.6(1)° (Table 1). In addition, a much smaller deviation between the central carbon atom (C1) and the plane defined by C2, C26, and C50 was observed in **CB-Mes-1** (0.030(3) Å), compared to **CB-Mes** (0.451(4) Å). The average C(central)–C(phenylene) bond length (**a**) shortens from 1.522(3) Å (**CB-Mes**) to 1.453(2) Å (**CB-Mes-1**), and the sum of the C–C1–C angle increases from 334.8(2)° (**CB-Mes**) to 359.9(2)° (**CB-Mes-1**). These results indicate that the central carbon atom is sp^3-hybridised in **CB-Mes**, but sp^2-hybridized in **CB-Mes-1**, as reported for unsubstituted $[CPh_3]^-$.[38] The average C(phenylene)–B bond appears to be slightly shortened from 1.553(6) Å in **CB-Mes** to 1.545(3) Å in **CB-Mes-1**, although the two values are within 3 esd's of one another. This value is slightly larger than that of linear boron-containing anions because, in **CB-Mes-1**, the electrons are distributed over the three $BMes_2$ groups.[29,40] This C(phenylene)–B bond is also longer than those in the one-electron-reduced 2-($BMes_2$)pyrene (1.514(6) Å) and the two-electron-reduced 2,7-bis($BMes_2$)pyrene (1.510(3) Å), in which the negative charge is predominantly localised on the boron centres, but is comparable to those observed in the one-electron-reduced species of the latter (1.547(6) Å) and in 1,4-bis($BMes_2$)phenylene (1.532(4) Å).[2] Compared to **CB-Mes**, the mean bond lengths **b** and **d** (Table 1; for labelling, see Fig. 2a) in **CB-Mes-1** become longer, whereas the average length of the **c** bonds decreases. Considering the short C(central)–C(phenylene) and C(phenylene)–B bonds and the significant C–C bond length alternation within the three phenyl rings, **CB-Mes-1** could be described as having a triple quinoidal structure. The optimised structures of **CB-Mes** and **CB-Mes-1** obtained from density functional theory (DFT) calculation show similar characteristics to those observed in their single crystal structures (Table 1).

As the NPh_3 core is isoelectronic with $[CPh_3]^-$, we selected model compounds N-(1,4-C_6H_4-BPh_2)$_3$ (**H**) and N-[1,4-C_6H_4–$B(C_6F_5)_2$]$_3$ (**I**)[31] as representative N-containing analogues (Fig. S4) for comparison. DFT, TD-DFT, and NBO calculations on **H** and **I** were conducted at the same level as for **CB-Mes′** and **CB-Mes-1′**, and the data are summarised in Table S3. The calculated **e** bond length in **CB-Mes-1′** (1.535 Å) is shorter than that in **H** (1.564 Å). In addition, the strong electron-withdrawing effect of the –C_6F_5 groups leads to a shortening of the **e** bond from 1.564 Å in **H** to 1.539 Å in **I**, whereas the C/$N_{central}$–$C_{phenylene}$ (**a**) bond lengths show only slight changes between **H** and **I**. These results indicate that the electron-donating ability of the central carbanion is significantly stronger than that of the N atom. Natural bond orbital (NBO) calculations reveal the presence of a C(phenylene)-to-B donor–acceptor interaction in **CB-Mes-1′** associated with a second-order energy of 150.7 kcal mol^{-1}. Consistent with these

structural trends, the Wiberg bond index (WBI) values of the **e** bond in **CB-Mes′** (0.908), **H** (0.918), and **I** (0.974) are all smaller than that in **CB-Mes-1′** (1.021). Moreover, the WBI value of the **a** bond (1.867) in **CB-Mes-1′** is almost twice those observed in **CB-Mes′** (0.986), **H** (1.013), and **I** (1.016). Natural population analysis (NPA) calculations on **CB-Mes** reveal that the charge on the boron atom is 0.881 e^-, which decreases to 0.802 e^- upon deprotonation. However, **H** and **I** exhibit boron charges that are 0.072 e^- and 0.079 e^-, respectively, more positive than that of **CB-Mes-1′**. These indicate increased electron densities in the C(phenylene)–B bonds and strong C(phenylene)–B interactions in **CB-Mes-1′**.

The torsion angles between the three phenyl rings in $[CPh_3]^-$ show significant differences (62.8(1)°, 51.9(1)°, and 43.8(1)°, Table S2) and, while two of them are fairly similar to that in **CB-Mes-1**, the third one is somewhat larger. Moreover, the bond lengths within the phenyl ring with the smallest torsion angle in $[CPh_3]^-$ exhibit a pronounced difference relative to the other two rings. These observations indicate that the electrons are not equally distributed among the three branches. In contrast, the three *p*-$BMes_2$ groups in **CB-Mes-1** exert a remarkable influence on the molecular geometry, enhancing the uniformity of electron delocalisation. Compared to $[CPh_3]^-$, **CB-Mes-1** exhibits decreased torsion angles and increased C–C bond length alternation in the three phenyl groups, attributed to its triple quinoidal resonance structure. In addition, the C(phenylene)–B bonds in **CB-Mes-1** are significantly shorter than those in linear donor-π-$BMes_2$ structures, such as (*p*-Me_2N-phenyl) dimesitylborane, illustrating that, although each boron center carries only one-third of the negative charge, the electron-donating ability of the carbanion is stronger than that of NMe_2.[41]

The harmonic oscillator model of aromaticity (HOMA) was calculated for **CB-Mes′** and **CB-Mes-1′** based on their DFT-optimised geometries to elucidate variations of aromaticity. The HOMA value of the central phenyl rings in **CB-Mes-1′** (0.82) is smaller than that in **CB-Mes′** (0.96), further verifying its triple quinoidal resonance structure.

Cyclic voltammetry (CV) and differential pulse voltammetry (DPV) measurements in THF (Fig. S5) reveal three reversible reductions at −2.72, −2.83, and −2.89 V (*vs.* Fc/Fc^+ in THF), which can be ascribed to the sequential reduction of the three $BMes_2$ groups in **CB-Mes**. The small redox potential gaps suggest a lack of substantial electron delocalisation in the neutral species. We also attempted to record the CV of **CB-Mes-1**; however, unfortunately, it is highly unstable in common electrolyte solutions such as $[^nBu_4N]^+[PF_6]^-$ and $[^nBu_4N]^+[B(C_6F_5)_4]^-$.

The UV-vis absorption spectra of **CB-Mes** and **CB-Mes-1** were measured in dry THF solutions under an argon atmosphere. **CB-Mes** shows two absorption bands in the ultraviolet region, with the maximum at 316 nm ($\varepsilon = 5.4 \times 10^4$ M^{-1} cm^{-1}), which results from the three $BMes_2$ groups (Fig. 3a and b).[42] Its fluorescence spectrum displays a single, broad emission band at 386 nm, with an absolute fluorescence quantum yield (Φ) of 0.23 in THF (Fig. 3c and Table S4). As the solvent polarity increases, the absorption of **CB-Mes** shows only slight changes, whereas the emission spectra exhibit a pronounced solvent-dependent behaviour, with the maximum shifting from 361 nm (hexane) to 399 nm (acetonitrile), indicating a charge transfer process in **CB-Mes**. For the anion **CB-Mes-1**, a broad absorption band is observed at 755 nm ($\varepsilon = ca.$ 10^4 M^{-1} cm^{-1}), which is significantly red-shifted compared to **CB-Mes**. This is attributed to its triple quinoidal resonance structure. Compared with calculated values for N-centred model compounds **H** and **I**, **CB-Mes-1** displays a significantly raised HOMO energy level (−2.89 eV *vs.* −7.19 eV for **H** and −8.21 eV for **I**; see Table S3), accompanied by a dramatic red shift of the maximum absorption band with a large oscillator strength.

Density functional theory (DFT) calculations on **CB-Mes′** and **CB-Mes-1′** were performed at the ωB97X-D/6-31G+(d,p) level (Fig. 4). For computational simplicity, the Mes groups in **CB-Mes** and **CB-Mes-1** were replaced with phenyl groups. Due to the C_3 symmetry of the optimised structures, the LUMO and LUMO + 1 of both molecules are degenerate and delocalised over the entire molecule. The HOMO of **CB-Mes′** is mainly localised on the three central phenyl rings with a small contribution from the central CH group, whereas in **CB-Mes-1′** there is a large contribution from the central carbon atom and delocalisation through the phenylene rings and onto the three boron atoms as well, further supporting the quinoidal structure. The HOMO of **CB-Mes-1′** is similar to that of $N[C_6H_4B(Mes)_2]_3$.[30,31,43] The

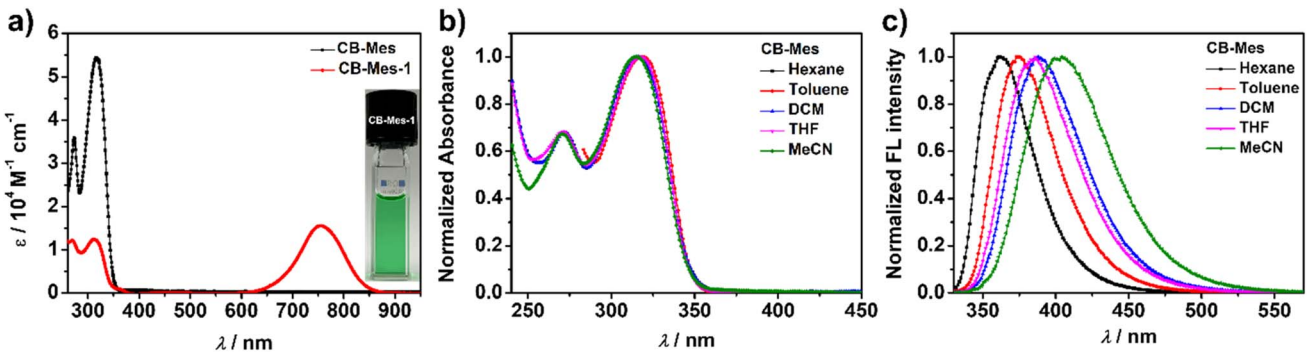

Fig. 3 (a) Absorption spectra of **CB-Mes** and **CB-Mes-1** in THF; (b) normalised absorption and (c) emission spectra of **CB-Mes** in different solvents.

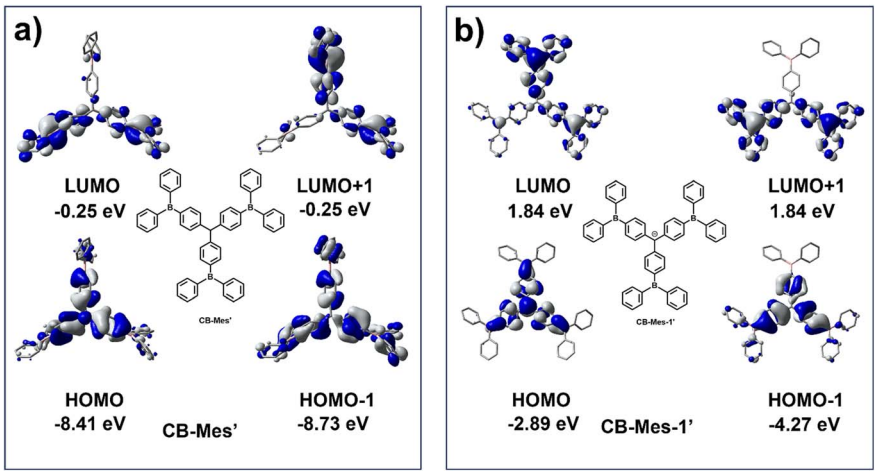

Fig. 4 Selected Kohn–Sham molecular orbitals and energy levels of (a) CB-Mes′ and (b) CB-Mes-1′.

positions of the absorption bands are accurately reproduced by time-dependent density functional theory (TD-DFT) calculations at the B3LYP/6-31+G(d,p) level. **CB-Mes′** (312 nm) and **CB-Mes-1′** (745 nm) exhibit strongly allowed transitions from S_0 to the lowest degenerate levels ($S_{1,2}$), which are attributed to the degenerate HOMO → LUMO and HOMO → LUMO + 1 transitions (Tables S5 and S6).

Conclusion

In summary, we have demonstrated that installing three strongly electron-accepting $BMes_2$ substituents at the *para*-positions of a trigonal CPh_3^- framework induces a remarkable structural and electronic evolution upon deprotonation of neutral **CB-Mes**. The resulting anion, **CB-Mes-1**, exhibits nearly similar geometries in its three branches, all of them showing shortened key C–C and C–B bonds and bond length alternation in the central phenyl rings, collectively indicative of a triple quinoidal delocalised structure. DFT calculations and spectroscopic evidence support an extensive redistribution of the negative charge over the entire π-framework, in stark contrast to the localised charge observed in classical CPh_3^- species in the solid state. In addition, this special geometry leads to a significant red shift (18 400 cm^{-1}) in the absorption of **CB-Mes-1**, formed by deprotonation of **CB-Mes**. These findings not only fill a missing conceptual gap regarding electron distribution in functionalised trigonal carbanions, but also provide a general molecular design principle for creating electronically adaptive anionic π-architectures.

Author contributions

T. B. M., L. J., and Y. Z. contributed to the conception and design of the experiments and wrote the manuscript. Y. Z. synthesized and characterized the compounds and conducted the photophysical measurements and theoretical studies. J. K. performed the single-crystal X-ray diffraction data collection and A. F. refined the structures and analysed the resulting data. I. K. performed the electrochemistry supervised by H. B. S. Y. provided valuable advice during data analysis and manuscript preparation and T. B. M., L. J., and S. Y. supervised the project. All authors analysed and discussed the results and participated in preparing the final draft of the manuscript.

Conflicts of interest

The authors declare no conflicts.

Data availability

The data supporting this article have been included as part of the supplementary information (SI). Supplementary information: including experimental details, synthesis, NMR spectra, UV-vis spectra, computational details, crystallographic information, and additional characterization data. See DOI: https://doi.org/10.1039/d5sc10121b.

CCDC 2504657 (for **CB-Mes**) and 2504659 (for **CB-Mes-1**) contain the supplementary crystallographic data for this paper.[44a,b]

Acknowledgements

We are grateful for generous financial support by the Nature Science Foundation of China (Grant No. 62174137), the Nature Science Basic Research Program of Shaanxi (Grant No. 2025JC-JCQN-047), the Fundamental Research Funds for the Central Universities, and Northwestern Polytechnical University. Y. Z gratefully acknowledges the China Scholarship Council for a scholarship to spend one year at Julius-Maximilians-Universität Würzburg and the Japan Society for the Promotion of Science (JSPS) (P25341) for a postdoctoral fellowship. T. B. M. thanks the Julius-Maximilians-Universität Würzburg for support. The authors thank Prof. Dr Bernd Engels (Julius-Maximilians-Universität) for helpful discussions regarding the DFT calculation and Prof. Dr John Evans (Durham University) for

helpful discussions regarding the calculation of standard uncertainty for averaged crystallographic values.

References

1 L. B. Ren, Y. Han, L. Y. Jiao, Y. Zou and J. S. Wu, Highly Strained, Fully π-Conjugated Porphyrin Cyclophanes: Template-Free Synthesis and Global Aromaticity, *Angew. Chem., Int. Ed.*, 2025, **64**, e202418532.
2 L. Ji, R. M. Edkins, A. Lorbach, I. Krummenacher, C. Brückner, A. Eichhorn, H. Braunschweig, B. Engels, P. J. Low and T. B. Marder, Electron Delocalisation in Reduced Forms of 2-($Bmes_2$)Pyrene and 2,7-Bis($Bmes_2$) Pyrene, *J. Am. Chem. Soc.*, 2015, **137**, 6750–6753.
3 Y. L. Wu, M. Frasconi, D. M. Gardner, P. R. McGonigal, S. T. Schneebeli, M. R. Wasielewski and J. F. Stoddart, Electron Delocalisation in a Rigid Cofacial Naphthalene-1,8:4,5-Bis(Dicarboximide) Dimer, *Angew. Chem., Int. Ed.*, 2014, **53**, 9476–9481.
4 T. Nishiuchi, S. Aibara and T. Kubo, Synthesis and Properties of a Highly Congested Tri(9-Anthryl)Methyl Radical, *Angew. Chem., Int. Ed.*, 2018, **57**, 16516–16519.
5 A. Das, B. J. Elvers, N. Chrysochos, S. K. I. Uddin, T. Gangber, I. Krummenacher, D. Borah, A. Mishra, M. Shanmugam, C. B. Yildiz, H. Braunschweig, C. Schulzke and A. Jana, Dianionic and Neutral Diboron-Centered Classical Diradicaloids, *J. Am. Chem. Soc.*, 2024, **146**, 9004–9011.
6 L. Wu, X. Zhang, M. Moos, I. Krummenacher, M. Dietz, A. Jayaraman, R. Bertermann, Q. Ye, M. Finze, M. Wenzel, R. Mitric, C. Lambert, H. Braunschweig and L. Ji, Full Electron Delocalisation across the Cluster in 1,12-Bis$Bmes_2$-*p*-Carborane Radical Anion, *J. Am. Chem. Soc.*, 2024, **146**, 17956–17963.
7 Z. Yuan, J. C. Collings, N. J. Taylor, T. B. Marder, C. Jardin and J. F. Halet, Linear and Nonlinear Optical Properties of Three-Coordinate Organoboron Compounds, *J. Solid State Chem.*, 2000, **154**, 5–12.
8 W. Kaim and A. Schulz, *p*-Phenylenediboranes: Mirror Images of *p*-Phenylenediamines, *Angew. Chem., Int. Ed.*, 1984, **23**, 615–616.
9 A. Schulz and W. Kaim, Bor-Organische Redoxsysteme, *Chem. Ber.*, 1989, **122**, 1863–1868.
10 J. Fiedler, S. Zalis, A. Klein, F. M. Hornung and W. Kaim, Electronic Structure of π-Conjugated Redox Systems with Borane/Borataalkene End Groups, *Inorg. Chem.*, 1996, **35**, 3039–3043.
11 S. Zalis and W. Kaim, Electronic Structures of Two Kinds of Oligoborane Radical Anions: Mixed-Valence Description of a Reduced p-Phenylenediborane and Spin Density Distributions in Distorted Octahedral Clusters $[B_6Hal_6]^{\bullet-}$, Hal = Cl, Br, I, *Main Group Chem.*, 2007, **5**, 267–276.
12 W. Kaim, N. S. Hosmane, S. Záliš, J. A. Maguire and W. N. Lipscomb, Boron Atoms as Spin Carriers in Two- and Three-Dimensional Systems, *Angew. Chem., Int. Ed.*, 2009, **48**, 5082–5091.
13 A. Lichtblau, W. Kaim, A. Schulz and T. Stahl, Organoboron Substituent Effects in EPR/ENDOR Spectroscopy. Radical Ions with B–C and B–N Bonds, *J. Chem. Soc., Perkin Trans. 2*, 1992, 1497–1501.
14 C. A. Coulson, Free Valence in Organic Reactions, *J. Chim. Phys. Phys.-Chim. Biol.*, 1948, **45**, 243–248.
15 P. Dowd, Trimethylenemethane, *J. Am. Chem. Soc.*, 1966, **88**, 2587–2589.
16 L. V. Slipchenko and A. I. Krylov, Electronic Structure of the Trimethylenemethane Diradical in Its Ground and Electronically Excited States: Bonding, Equilibrium Geometries, and Vibrational Frequencies, *J. Chem. Phys.*, 2003, **118**, 6874–6883.
17 K. Komaguchi, M. Shiotani and A. Lund, An ESR Study of Trimethylenemethane Radical Cation, *Chem. Phys. Lett.*, 1997, **265**, 217–223.
18 S. Baghery, M. Zarei, M. A. Zolfigol, S. Mallakpour and V. Behranvand, Application of Trityl Moieties in Chemical Processes: Part I, *J. Iran. Chem. Soc.*, 2020, **17**, 2737–2843.
19 B. M. Trost, [3+2] Cycloaddition Approaches to 5-Membered Rings Via Trimethylenemethane and Its Equivalents, *Angew. Chem., Int. Ed.*, 1986, **25**, 1–20.
20 J. S. Alexander and K. Ruhlandt-Senge, Barium Triphenylmethanide: An Examination of Anion Basicity, *Angew. Chem., Int. Ed.*, 2001, **40**, 2658–2660.
21 M. Gomberg, An Instance of Trivalent Carbon Triphenylmethyl, *J. Am. Chem. Soc.*, 1900, **22**, 757–771.
22 H. Nishimae, H. Kurata and M. Oda, Arylbis(9-Anthryl) Methyl Cations: Highly Crowded, near Infrared Light Absorbing Hydrocarbon Cations, *Angew. Chem., Int. Ed.*, 2004, **43**, 4947–4950.
23 S. Harder, S. Müller and E. Hübner, Syntheses and Crystal Structures of Simple Dibenzylcalcium Complexes: Useful Reagents in the Preparation of Calcium Compounds, *Organometallics*, 2004, **23**, 178–183.
24 M. M. Olmstead and P. P. Power, The Isolation and X-Ray Structures of Lithium Crown Ether Salts of the Free Phenyl Carbanions $[CHPh_2]^-$ and $[CPh_3]^-$, *J. Am. Chem. Soc.*, 1985, **107**, 2174–2175.
25 D. E. Smiles, G. Wu and T. W. Hayton, Synthesis of Uranium-Ligand Multiple Bonds by Cleavage of a Trityl Protecting Group, *J. Am. Chem. Soc.*, 2014, **136**, 96–99.
26 S. Harder, Schlenk's Early "Free" Carbanions, *Chem.–Eur. J.*, 2002, **8**, 3229–3232.
27 S. Lovell, B. J. Marquardt and B. Kahr, Crystal Violet's Shoulder, *J. Chem. Soc., Perkin Trans. 2*, 1999, 2241–2247.
28 R. Stahl, C. Lambert, C. Kaiser, R. Wortmann and R. Jakober, Electrochemistry and Photophysics of Donor-Substituted Triarylboranes: Symmetry Breaking in Ground and Excited State, *Chem.–Eur. J.*, 2006, **12**, 2358–2370.
29 P. Y. Feng, Y. H. Liu, T. S. Lin, S. M. Peng and C. W. Chiu, Redox Chemistry of a Hydroxyphenyl-Substituted Borane, *Angew. Chem., Int. Ed.*, 2014, **53**, 6237–6240.
30 N. S. Makarov, S. Mukhopadhyay, K. Yesudas, J.-L. Brédas, J. W. Perry, A. Pron, M. Kivala and K. Müllen, Impact of Electronic Coupling, Symmetry, and Planarization on One- and Two-Photon Properties of Triarylamines with One, Two, or Three Diarylboryl Acceptors, *J. Phys. Chem. A*, 2012, **116**, 3781–3793.

31 R. F. Jin, X. F. Zhang, W. M. Xiao and D. M. Luo, Theoretical Investigations of the Photophysical Properties of Star-Shaped π-Conjugated Molecules with Triarylboron Unit for Organic Light-Emitting Diodes Applications, *Int. J. Mol. Sci.*, 2017, **18**, 2178.

32 J. C. Doty, B. Babb, P. J. Grisdale, M. Glogowski and J. L. R. Williams, Boron Photochemistry IX. Synthesis and Fluorescent Properties of Dimesityl-Phenylboranes, *J. Organomet. Chem.*, 1972, **38**, 229–236.

33 C. D. Entwistle and T. B. Marder, Boron Chemistry Lights the Way: Optical Properties of Molecular and Polymeric Systems, *Angew. Chem., Int. Ed.*, 2002, **41**, 2927–2931.

34 C. D. Entwistle and T. B. Marder, Applications of Three-Coordinate Organoboron Compounds and Polymers in Optoelectronics, *Chem. Mater.*, 2004, **16**, 4574–4585.

35 L. Ji, S. Griesbeck and T. B. Marder, Recent Developments in and Perspectives on Three-Coordinate Boron Materials: A Bright Future, *Chem. Sci.*, 2017, **8**, 846–863.

36 S. Y. Li, Z. B. Sun and C. H. Zhao, Charge-Transfer Emitting Triarylborane π-Electron Systems, *Inorg. Chem.*, 2017, **56**, 8705–8717.

37 A. Wakamiya and S. Yamaguchi, Designs of Functional π-Electron Materials Based on the Characteristic Features of Boron, *Bull. Chem. Soc. Jpn.*, 2015, **88**, 1357–1377.

38 G. Li, W. B. Yang, S. H. Wang, T. Liu, C. Q. Yan, G. Li, Y. Zhang, D. D. Li, X. Y. Wang, P. Hao, J. W. Li, L. J. Huo, H. Yan and B. Tang, Methane-Perylene Diimide-Based Small Molecule Acceptors for High Efficiency Non-Fullerene Organic Solar Cells, *J. Mater. Chem. C*, 2019, **7**, 10901–10907.

39 C. Kleeberg, On the Structural Diversity of K(18-Crown-6) EPh_3 Complexes (E = C, Si, Ge, Sn, Pb): Synthesis, Crystal Structures and NOESY NMR Study, *Dalton Trans.*, 2013, **42**, 8276–8287.

40 M. M. Olmstead, P. P. Power, K. J. Weese and R. J. Doedens, Isolation and X-Ray Crystal-Structure of the Boron Methylidenide Ion $[Mes_2BCH_2]^-$ (Mes = 2,4,6-$Me_3C_6H_2$): A Boron-Carbon Double Bonded Alkene Analog, *J. Am. Chem. Soc.*, 1987, **109**, 2541–2542.

41 Z. Yuan, C. D. Entwistle, J. C. Collings, D. Albesa-Jové, A. S. Batsanov, J. A. K. Howard, N. J. Taylor, H. M. Kaiser, D. E. Kaufmann, S. Y. Poon, W. Y. Wong, C. Jardin, S. Fathallah, A. Boucekkine, J.-F. Halet and T. B. Marder, Synthesis, Crystal Structures, Linear and Nonlinear Optical Properties, and Theoretical Studies of (*p*-R-Phenyl)-, (*p*-R-Phenylethynyl)-, and (*E*)-2-(*p*-R-Phenyl)Ethenyl Dimesitylboranes and Related Compounds, *Chem.–Eur. J.*, 2006, **12**, 2758–2771.

42 M. E. Long, Absorption and Emission of Substituted Dimesitylboranes, *J. Lumin.*, 1978, **16**, 177–189.

43 For a related study of dipolar, quadrupolar, and octupolar amino donor – $B(Mes)_2$ acceptor systems and their one- and two-photon optical properties, see: J. C. Collings, S.-Y. Poon, C. Le Droumaguet, M. Charlot, C. Katan, L. O. Pålsson, A. Beeby, J. A. Mosely, H. M. Kaiser, D. E. Kaufmann, W.-Y. Wong, M. Blanchard-Desce and T. B. Marder, The Synthesis and One- and Two-Photon Optical Properties of Dipolar, Quadrupolar and Octupolar Donor-Acceptor Molecules Containing Dimesitylboryl Groups, *Chem.–Eur. J.*, 2009, **15**, 198–208.

44 (*a*) CCDC 2504657: Experimental Crystal Structure Determination, 2026, DOI: 10.5517/ccdc.csd.cc2q29dj; (*b*) CCDC 2504659: Experimental Crystal Structure Determination, 2026, DOI: 10.5517/ccdc.csd.cc2q29gl.